Variational Monte Carlo calculations of ground states of liquid ^{4}He and ^{3}He drops

V. R. Pandharipande
Department of Physics and Materials Research Laboratory, University of Illinois, Urbana, Illinois 61801

Steven C. Pieper and R. B. Wiringa
Physics Division, Argonne National Laboratory, Argonne, Illinois 60439-4843

(Received 13 March 1986)

Variational Monte Carlo calculations of the ground states of drops containing 8—728 atoms of ^{4}He and 20—240 atoms of ^{3}He have been made. The variational wave functions include two- and three-body correlations and (for the Fermi drops) Feynman-Cohen backflow. We discuss the wave functions, their relation to modern variational wave functions for liquid ^{4}He and ^{3}He, the calculational techniques, and the results for the ground-state energies and density profiles. Our calculations indicate that ^{3}He drops with more than 40 atoms are bound, while a drop with 20 atoms is in a metastable state that has positive energy but negative chemical potential. The surface tensions of both liquid ^{4}He and ^{3}He are obtained by liquid-drop fits to the calculated binding energies. From the density profiles of the largest drops we estimate the surface thickness of liquid ^{4}He to be 7 Å while that for liquid ^{3}He is 8 Å.

I. INTRODUCTION

In the past few years the ground-state properties of both Bose liquid ^{4}He and Fermi liquid ^{3}He have been successfully calculated from a quantum-mechanical Hamiltonian containing the HFDHE2 potential of Aziz *et al.*[1] More recently, we have calculated the ground-state properties of finite drops of these liquids from the same Hamiltonian, with the variational Monte Carlo (VMC) method. A brief report of the calculations of the liquid-^{4}He drops was published earlier;[2] this paper presents a more complete version of that work and the first results for ^{3}He drops. From theoretical studies it appears that any number of ^{4}He atoms form a bound state; however, only those with more than ten atoms have radii which increase approximately as $N^{1/3}$, where N denotes the number of atoms. Since we expect the radius of a liquid drop to be proportional to $N^{1/3}$, we may refer to bound states of more than ten ^{4}He atoms as liquid drops. A significant finding of the present study is that a large number of ^{3}He atoms are needed to form a bound drop with negative energy. Our calculations indicate that drops with $N \gtrsim 40$ are bound, while ~ 20 atoms form a metastable state that has positive energy but negative chemical potential. The lighter mass of the ^{3}He atom and its fermion nature are responsible for this behavior. For example, eight ^{3}He atoms would form a bound state if they were bosons, and eight ^{4}He atoms would be bound even if they were fermions, but eight ^{3}He fermions do not form a bound state.

Quantum liquid drops are simple examples of inhomogeneous quantum systems, and are of interest in both nuclear and condensed-matter physics. The binding energy, surface tension, and density of the liquid can be obtained by fitting the energy per particle $e(N)$ and the radius $R(N)$ of drops with N particles with power series in $N^{1/3}$. The thickness of the liquid surface can also be estimated from the density profiles of large drops. While the helium-liquid properties are known experimentally, the idealized nuclear matter properties can only be deduced in this manner. Our studies of liquid-helium drops suggest this kind of extrapolation is valid but also indicate difficulties with the procedure. Drops of liquid ^{3}He and ^{4}He have been studied with phenomenological energy-density functionals.[3,4] We hope that the present microscopic calculations will be useful in obtaining a better understanding of these simpler approaches to the theory of inhomogeneous quantum systems. Local-density approximations[4,5] are also frequently used in the theory of liquid-helium surfaces. Their validity can be tested with the present microscopic calculations.

The variational wave functions used in the present study of the drops are generalizations of those used in the study of helium liquids.[6–9] In Sec. II we give a brief review of the theory of helium liquids; the variational wave functions of the drops are given in Sec. III. The details of the Monte Carlo calculations are given in Sec. IV, and the results are presented in Sec. V.

II. VARIATIONAL THEORY OF HELIUM LIQUIDS

Liquid ^{4}He has been studied with the Hamiltonian:

$$H = \sum_{i=1}^{N} \left[-\frac{\hbar^2}{2m} \nabla_i^2 \right] + \sum_{\substack{i,j \\ i<j\le N}} v(r_{ij}) , \tag{2.1}$$

using the variational wave function:[6,7]

$$\Psi(\mathbf{R}) = \prod_{\substack{i,j \\ i<j\le N}} f_2(r_{ij}) \prod_{\substack{i,j,k \\ i<j<k\le N}} f_3(r_{ij}, r_{jk}, r_{ki}) , \tag{2.2}$$

in the limit $N\to\infty$ at constant density. Here $v(r_{ij})$ is the Aziz HFDHE2 interatomic potential[1] and we use the $3N$-dimensional vector $\mathbf{R}$ to denote $\mathbf{r}_1,\mathbf{r}_2,\ldots,\mathbf{r}_N$. In principle the coupled Euler-Lagrange equations

$$\frac{\delta\langle H\rangle}{\delta f_2}=0\ , \tag{2.3}$$

$$\frac{\delta\langle H\rangle}{\delta f_3}=0\ , \tag{2.4}$$

should be solved to determine the pair and triplet correlations f_2 and f_3. However, this has not yet been achieved with sufficient accuracy. By setting $f_3=1$ (Jastrow approximation), and using the lowest-order hypernetted-chain (HNC/0) expression for $\langle H\rangle$ with the Jackson-Feenberg kinetic energy (we denote this set of approximations by J-HNC/0-JF), Eq. (2.3) has been solved by Campbell and Feenberg,[10] and more recently by Lantto and Siemens.[11] In this approximation they obtain an equation for the pair distribution function $g(r)$,

$$\left[-\frac{\hbar^2}{m}\nabla^2+v(r)+\omega(r)\right]\sqrt{g(r)}=0\ . \tag{2.5}$$

The $g(r)$ is a functional of f_2 and the liquid density ρ, and the induced potential $\omega(r)$ is a known functional of $g(r)$ and f_2. Equation (2.5) can thus be solved iteratively. Unfortunately, the J-HNC/0-JF approximation is rather poor; one obtains, with it and the Aziz potential, the energy $e_0=-5.35$ K per atom at an equilibrium density $\rho_0=0.017$ Å^{-3}. The experimental value is -7.14 K at 0.0219 Å^{-3}, while the value obtained with the Aziz potential and the exact Green's-function Monte Carlo (GFMC) method[12] is -7.11 K at 0.022 Å^{-3}.

The variational procedure of Refs. 13 and 6 makes use of very general arguments[14] that relate the long-range behavior of f_2 to the speed of sound, c, in the liquid:

$$f_2(r\to\infty)=1-\alpha/r^2\ , \tag{2.6}$$

$$\alpha=\frac{mc}{2\pi^2\hbar\rho}\ . \tag{2.7}$$

This asymptotic behavior of f_2 is obtained by choosing a matching radius d and taking $f_2(r>d)$ from Eq. (2.6). A constant λ_ω is added to the induced potential, so that Eq. (2.5) becomes

$$\left[-\frac{\hbar^2}{m}\nabla^2+v(r)+\omega(r)+\lambda_\omega\right]\sqrt{g(r)}=0\ , \tag{2.8}$$

and λ_ω is chosen to obtain an f_2 continuous at $r=d$. The λ_ω is meant to correct the errors in the calculation of $\omega(r)$ with the J-HNC/0-JF approximation. Equations (2.6) and (2.8) and the J-HNC/0-JF equations define a family of pair correlation functions f_2 with parameters ρ and α. In Ref. 6, these parameters are fixed by consistency; the physical density of the liquid gives the ρ, and α is taken from Eq. (2.7).

Chang and Campbell[15] have attempted to solve Eq. (2.4) for the correlation f_3. However, in Refs. 6, 7, and 13, the correlation f_3 is described by a simple, theoretically plausible, algebraic expression having a few parameters. The functional form used in Ref. 6 is

$$f_3(r_{ij},r_{jk},r_{ki})=\exp\left[-\tfrac{1}{2}\sum_{\text{perm}}\sum_l \xi_l(r_{ij})\xi_l(r_{ik})r_{ij}^l r_{ik}^l P_l(\cos\theta_i)\right]\ , \tag{2.9}$$

where $\sum_{\text{perm}}$ contains the three cyclic permutations of i, j, and k, and θ_i is the angle between $\mathbf{r}_{ij}$ and $\mathbf{r}_{ik}$. The $l=1$ term of f_3 is the most important, and it lowers e_0 by ~ 1 K. The $l=0$ and 2 terms have been included in the calculations of Ref. 6; they have small effects. The $l=0$ and 1 $\xi_l(r)$ are parametrized as follows:

$$\xi_0(r)=(\lambda_{\xi_0})^{1/2}(r-r_{\xi_0})\exp\{-[(r-r_{\xi_0})/\omega_{\xi_0}]^2\}\ , \tag{2.10}$$

$$\xi_1(r)=(\lambda_{\xi_1})^{1/2}\exp\{-[(r-r_{\xi_1})/\omega_{\xi_1}]^2\}\ , \tag{2.11}$$

and the λ_{ξ_l}, r_{ξ_l}, and ω_{ξ_l} are varied to minimize the energy. The f_3 influences the compressibility of the liquid, and thus the α [Eq. (2.7)]. Hence in Ref. 6 the f_2 and f_3 are determined together consistently. These variational calculations give $e_0=-6.89$ K at $\rho_0=0.0217$ Å^{-3}.

Modern variational calculations[8,9] of liquid ^{3}He use the wave function:

$$\psi(\mathbf{R})=\prod_{\substack{i,j\\ i<j\le N}} f_2(r_{ij})\prod_{\substack{i,j,k\\ i<j<k\le N}} f_3(r_{ij},r_{jk},r_{ki})\times\prod_{\substack{i,j\\ i<j\le N}} f_{\text{bf}}(ij)\Phi(\mathbf{R})\ , \tag{2.12}$$

in the limit $N\to\infty$ at constant density. Here Φ is the Fermi-gas wave function

$$\Phi(\mathbf{R})=||\phi_i(\mathbf{r}_j)||\ , \tag{2.13}$$

$$\phi_i(\mathbf{r}_j)=\exp(i\mathbf{k}_i\cdot\mathbf{r}_j)\ , \tag{2.14}$$

where we have suppressed the spin functions for brevity. The $f_{\text{bf}}(ij)$ are Feynman-Cohen backflow[16] correlations, and their effect is most conveniently expressed as[9]

$$\prod_{\substack{i,j\\ i<j\le N}} f_{\text{bf}}(ij)\Phi(\mathbf{R})=\Phi(\mathbf{R}')=||\phi_i(\mathbf{r}_j')||\ , \tag{2.15}$$

$$\mathbf{r}_i'=\mathbf{r}_i+\sum_j \eta(r_{ij})(\mathbf{r}_i-\mathbf{r}_j)\ . \tag{2.16}$$

In Ref. 8 the f_2 is taken from the ^{3}He Bose liquid, and only the $l=1$ term of the f_3 [Eq. (2.9)] is retained. The $\eta(r)$ is taken as

$$\eta(r)=\lambda_\eta\exp\{-[(r-r_\eta)/\omega_\eta]^2\}\ , \tag{2.17}$$

and λ_{ξ_1}, r_{ξ_1}, ω_{ξ_1}, λ_η, r_η, and ω_η are varied to minimize the energy. The calculations use Fermi hypernetted-chain (FHNC) summation methods, which are expected to have

an accuracy of ~ 0.1 K, and give an equilibrium point having $e_0 = -2.36$ K at $\rho_0 = 0.0174$ Å^{-3}. The experimental value is -2.47 K at 0.0165 Å^{-3}. Recent VMC and GFMC calculations have been done only at $\rho = 0.0165$ Å^{-3}. The variational calculations,[17] using a wave function similar to that used in Ref. 8, give $e = -2.15 \pm 0.05$ K. GFMC calculations with fixed nodes[18] give $e = -2.33$ K, while transient estimates[18] give $e = -2.44 \pm 0.04$ K. Exact fermion GFMC calculations are not yet possible.

The effects of several simplifications of the variational wave function have been studied in Ref. 8. If backflow is neglected [$\eta(r) = 0$], the energy at $\rho = 0.0166$ Å^{-3} goes up from -2.36 to -1.83 K. If both $f_{\rm bf}$ and f_3 are neglected (Jastrow approximation) it goes up to -1.28 K. Lowest-order FHNC calculations using Jastrow wave functions and the Jackson-Feenberg kinetic energy (the J-FHNC/0-JF approximation) give $e = -0.52$ K at $\rho = 0.0166$ Å^{-3}.

III. VARIATIONAL WAVE FUNCTIONS FOR LIQUID-HELIUM DROPS

Three different parametrizations, denoted Ψ_A, Ψ_B, and Ψ_C, of the variational wave function were used for liquid-^{4}He drops. Both Ψ_A and Ψ_B have the form ($x = A, B$):

$$\psi_x = \prod_{\substack{i,j,k \\ i<j<k\le N}} f_3(r_{ij}, r_{jk}, r_{ki}) \times \prod_{\substack{i,j \\ i<j\le N}} f_2(r_{ij}) \prod_{i \le N} f_{1,x}(r_i) \, . \tag{3.1}$$

The $f_{1,A}$ is taken as the ground-state wave function of a particle in a Woods-Saxon potential well:

$$\left[-\frac{\hbar^2}{2\mu} \nabla^2 + U(r) \right] f_{1,A}(r) = e_\phi f_{1,A}(r) \, , \tag{3.2}$$

$$\mu = \frac{N-1}{N} m \, , \tag{3.3}$$

$$U(r) = V_\phi \{ 1 + \exp[(r - r_\phi)/\omega_\phi] \}^{-1} \, , \tag{3.4}$$

while $f_{1,B}$ is taken as the Fermi function,

$$f_{1,B}(r) = \{ 1 + \exp[(r - r_\phi)/\omega_\phi] \}^{-1} \, . \tag{3.5}$$

The parameters r_ϕ and ω_ϕ (and V_ϕ of $f_{1,A}$) are varied to minimize the energy. The Bose liquid $f_2(\alpha, \rho_L)$ obtained from Eqs. (2.6) and (2.8) is used; however, the α and ρ_L are treated strictly as variational parameters to minimize the energy, and they have no physical significance. The f_3 has the functional form (2.9), and only the $l = 0$ and 1 terms are retained. The $\xi_l(r)$ are given by Eqs. (2.10) and (2.11), and the λ_{ξ_0} and λ_{ξ_1} are varied to minimize the energy. We attempted to vary r_{ξ_l} and ω_{ξ_l} also, but found that these parameters have equilibrium values close to those in the extended liquid.

The wave functions Ψ_A and Ψ_B are not translationally invariant, and the kinetic energy associated with the center-of-mass motion,

$$\left\langle \left[\frac{-\hbar^2}{2mN} \right] \left[\sum_{i=1}^{N} \nabla_i \right]^2 \right\rangle ,$$

has to be subtracted from $\langle H \rangle$. We find that Ψ_A is variationally better for drops with $N > 70$ atoms, while Ψ_B is better for drops having $20 \le N < 70$ atoms. We cannot determine which is better for $N = 70$. The translationally invariant wave function

$$\Psi_C = \prod_{\substack{i,j,k \\ i<j<k\le N}} f_3(r_{ij}, r_{jk}, r_{ki}) \prod_{\substack{i,j \\ i<j\le N}} \tilde{f}_2(r_{ij}) \, , \tag{3.6}$$

gives lower binding energies for systems with less than ten atoms. The $\tilde{f}_2(r)$ in Ψ_C has the asymptotic behavior:

$$\tilde{f}_2(r \to \infty) = e^{-\kappa r} r^{-1/(N-1)} \, , \tag{3.7}$$

appropriate for a bound system.[19] The $\tilde{f}_2$ is taken to be the solution of

$$\left[-\frac{\hbar^2}{m} \nabla^2 + v(r) + \lambda(r) \right] \tilde{f}_2(r) = 0 \, , \tag{3.8}$$

$$\lambda(r) = \frac{\hbar^2}{m} \left[\kappa^2 - 2 \left[\frac{N-2}{N-1} \right] \frac{\kappa}{r} - \frac{1}{N-1} \left[\frac{N-2}{N-1} \right] \frac{1}{r^2} \right] \times \{ 1 - \exp[-(r/C)^2] \} + \gamma_\lambda \{ 1 + \exp[(r - r_\lambda)/\omega_\lambda] \}^{-1} \, , \tag{3.9}$$

and the parameters κ, r_λ, ω_λ, and C are varied while γ_λ is fixed by requiring the f_2 to be finite at $r = 0$. The f_3 in Ψ_C has the same form as that in Ψ_A or Ψ_B.

The main simplifying assumption in these variational wave functions is that the f_2 and f_3 are functions of interparticle distances only. In general, the pair correlation f_2 in an inhomogeneous system, like a liquid drop, can depend on $\mathbf{r}_i$ and $\mathbf{r}_j$, and not just the distance r_{ij}. However, this approximation should be good at small r_{ij} where the f_2 is dominated by the strong two-body potential $v(r_{ij})$. It is well known that the liquid energy is insensitive to how one lets f_2 go to unity at $r_{ij} > 3$ Å. For example, the McMillan f_2,

$$f_2(r) = \exp[-\tfrac{1}{2}(b/r)^5] \, , \tag{3.10}$$

has the correct behavior at small r when the Lennard-Jones potential is used. It does not have the $1 - \alpha/r^2$ tail of the optimum f_2. However, the liquid energies obtained for the Lennard-Jones potential at $\rho = 0.0217$ Å^{-3}, with the McMillan and the optimum f_2 are, respectively, -5.7 and -5.85 K per atom when $f_3 = 1$. We can hope that the gross properties of the drops are also relatively insensitive to the long-range behavior of f_2.

We have recently studied[20] the frequencies of compression (breathing mode), and the surface (ripplon) vibrations of liquid-^{4}He drops with variational wave functions of the type used by Chang and Cohen,[5] based on the ground-state Ψ_A and Ψ_B. Reasonable results are obtained when the vibrational energies are > 2 K; however, the very-

low-energy surface modes are not properly described. The frequencies of these modes are determined by very-long-range correlations among surface particles, which these wave functions do not appear to simulate correctly.

Recently, Krotscheck, Qian, and Kohn[21] have developed a theory of inhomogeneous quantum systems based on a variational wave function in which $f_3=1$ and f_2 is a function of $\mathbf{r}_i$ and $\mathbf{r}_j$. In essence, they generalize the J-HNC/0-JF method to inhomogeneous systems. Due to the approximations in this method, the gross results they obtain are not very accurate; the calculated surface tension (0.14 K Å^{-2}) is approximately half the correct value, and the liquid binding energy and density are also wrong by $\sim 30\%$. However, pursuit of such semianalytic approaches may give new insight into the large-distance behavior of f_2 in inhomogeneous systems which can be incorporated into the variational wave functions.

The variational wave function of the Fermi-liquid-^{3}He drops is taken to be

$$\Psi = \prod_{\substack{i,j,k \\ i<j<k\le N}} f_3(r_{ij},r_{jk},r_{ki}) \prod_{\substack{i,j \\ i<j\le N}} f_2(r_{ij})\Phi \,, \tag{3.11}$$

$$\Phi = \Phi_\uparrow(\mathbf{r}'_1,\ldots,\mathbf{r}'_{N/2})\Phi_\downarrow(\mathbf{r}'_{N/2+1},\ldots,\mathbf{r}'_N) \,, \tag{3.12}$$

$$\Phi_\uparrow = ||\phi_i(\mathbf{r}'_j)||\chi_\uparrow(1)\cdots\chi_\uparrow(N/2) \,, \tag{3.13}$$

$$\Phi_\downarrow = ||\phi_i(\mathbf{r}'_j)||\chi_\downarrow(N/2+1)\cdots\chi_\downarrow(N) \,. \tag{3.14}$$

The determinants $\Phi_\uparrow$ and $\Phi_\downarrow$ are of order $N/2$ with $1\le i\le N/2$ in both cases and $1\le j\le N/2$ in $\Phi_\uparrow$ and $N/2+1\le j\le N$ in $\Phi_\downarrow$. The $\chi_{\uparrow,\downarrow}$ are spin functions which we will omit for brevity. The $\phi_i(\mathbf{r})$ are the lowest $N/2$ states of a particle of mass $m(N-1)/N$ in the Woods-Saxon potential well given by Eq. (3.4). The r_ϕ, ω_ϕ, and V_ϕ are varied to minimize the energy.

It is well known in nuclear physics that Fermi-liquid drops can have intrinsic deformations due to shell effects.[22] We want to avoid these complications at this stage, and hence use the above wave function for only the "closed shell" values $N=8$, 20, 40, 70, 112, 168, and 240. At these values of N the Fermi energy in a spherically symmetric Woods-Saxon well has large gaps, and hence the choice of single-particle levels to be included in the Φ is unambiguous.

The f_2 and f_3 are parametrized as for the ^{4}He drops, and the $\mathbf{r}'_i$ are related to the $\mathbf{r}_i$ by Eq. (2.16). The backflow function $\eta(r)$ should in principle have a $1/r^3$ tail,[16] and in the study of elementary excitations of liquid ^{4}He this long-range $\eta(r)$ is found to be variationally superior.[23] However, only short-range $\eta(r)$ [Eq. (2.17)] have been used in the calculations of extended liquid ^{3}He due to technical difficulties. There is no difficulty in using long-range $\eta(r)$ in the finite drops, and hence the $\eta(r)$ is parametrized as

$$\eta(r) = \lambda_\eta \exp\{-[(r-r_\eta)/\omega_\eta]^2\} + \lambda'_\eta/r^3 \,. \tag{3.15}$$

We found the lowest energies for $\lambda_\eta=0$ and $\lambda'_\eta\neq 0$; however, the difference from the energy obtained with $\lambda_\eta\neq 0$ and $\lambda'_\eta=0$ is much smaller than the total effect of the backflow correlations on the energy.

IV. THE MONTE CARLO CALCULATIONS

A. Metropolis random walk

The variational estimate of the bound-state energy for a given trial wave function is given by

$$E = \langle\Psi|H|\Psi\rangle/\langle\Psi|\Psi\rangle \,, \tag{4.1}$$

$$= \int d\mathbf{R}\, P(\mathbf{R})H(\mathbf{R}) \,, \tag{4.2}$$

where

$$P(\mathbf{R}) = |\Psi(\mathbf{R})|^2 \Big/ \int d\mathbf{R}\,|\Psi(\mathbf{R})|^2 \,, \tag{4.3}$$

and

$$H(\mathbf{R}) = \frac{1}{\Psi(\mathbf{R})} H\Psi(\mathbf{R}) \,. \tag{4.4}$$

Equation (4.2) has the form of a probability integral with the probability function $P(\mathbf{R})$. We use the method of Metropolis[24] to evaluate this integral. In this method, a random walk, governed by $P(\mathbf{R})$, is made in the space $\mathbf{R}$. At each step of the walk, the function $H(\mathbf{R})$ is evaluated and the average of these values is an estimate of the integral (4.2).

To make one step of the random walk, one can attempt to move all the particles at once, or one can move them one at a time. The very strong short-range repulsion of the interatomic potential creates a significant volume in which $P(\mathbf{R})$ is essentially zero, and hence the probability of accepting a move in which all the particles change position decreases as N^{-2} [only one pair of particles has to get close together to make $P(\mathbf{R})$ small]. This problem can be avoided by using molecular dynamics to move the particles; however, we simply move one particle at a time with an average step size (1.2–2 Å) chosen to give an acceptance rate of 50%. Typically, $5N$ one-particle moves are used to generate one step of the random walk.

If the values of $H(\mathbf{R})$ obtained in this random walk have a normal distribution, the standard deviation of the mean of the values

$$\delta = \sigma/(N_{\rm step})^{1/2} \,, \tag{4.5}$$

where

$$\sigma^2 = \left[\sum_i [H(\mathbf{R}_i)/N - E/N]^2\right] \Big/ N_{\rm step} \,, \tag{4.6}$$

is an estimate of the statistical error in the evaluation of the integral. (The δ and σ are defined in terms of the energy per atom for later convenience.) We find that the distribution of the $H(\mathbf{R})$ is not normal, but rather is sharply peaked with long tails (Fig. 1). A normal distribution may be produced by averaging groups (of about 50 each) of the $H(\mathbf{R})$'s and these partial averages can be used to compute the standard deviation. However, it turns out that the resulting standard deviation is not substantially different from the simple standard deviation of the $H(\mathbf{R})$'s.

The kinetic-energy part, $T(\mathbf{R})$, of $H(\mathbf{R})$ can be evaluated in different ways by performing integrations by parts.[25,26] The commonly used forms are the Pandharipande-Bethe form,

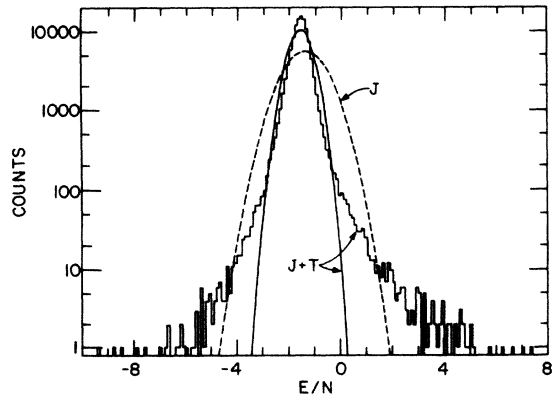

FIG. 1. Histogram (on a logarithmic scale) of 110000 values of $H(\mathbf{R})/N$ for the 20-atom ^{4}He drop. The solid curve is the Gaussian with the same mean value and standard deviation. The dashed curve is the corresponding Gaussian for a calculation in which the triplet correlation is eliminated.

$$T_{\rm PB}(\mathbf{R})=\sum_{i=1}^{N}\left[-\frac{\hbar^2}{2m}\right]\frac{1}{\Psi(\mathbf{R})}\nabla_i^2\Psi(\mathbf{R})\ , \tag{4.7}$$

the Clark-Westhaus form,

$$T_{\rm CW}(\mathbf{R})=\sum_{i=1}^{N}\frac{\hbar^2}{2m}\frac{1}{|\Psi(\mathbf{R})|^2}\nabla_i\Psi^*(\mathbf{R})\cdot\nabla_i\Psi(\mathbf{R})\ , \tag{4.8}$$

and the Jackson-Feenberg form,

$$T_{\rm JF}(\mathbf{R})=\tfrac{1}{4}[2T_{\rm CW}(\mathbf{R})+T_{\rm PB}(\mathbf{R})+T_{\rm PB}^*(\mathbf{R})]\ . \tag{4.9}$$

We find that the smallest standard deviation is obtained by using $T_{\rm PB}(\mathbf{R})$ because if $\Psi(\mathbf{R})$ is an eigenstate of H, then all the values of $H(\mathbf{R})$ obtained with the $T_{\rm PB}(\mathbf{R})$ would equal the eigenvalue E, and there would be no deviation. The integration by parts used in $T_{\rm CW}$ and $T_{\rm JF}$ destroys this eigenvalue property. The statistical error in the evaluation of the integral is typically larger by a factor of 5.5 (11) when $T_{\rm JF}$ ($T_{\rm CW}$) is used instead of $T_{\rm PB}$. All the results reported here are obtained with $T_{\rm PB}$. In order to avoid the extensive algebra that would be involved in calculating $\nabla_i^2\Psi$ in terms of the derivatives of f_1, f_2, f_3, η, and the ϕ_i's, the $\nabla_i^2\Psi$ are computed numerically by evaluating differences of $\Psi(\mathbf{R})$ for small displacements of the particles.

Because of the eigenvalue property of $H(\mathbf{R})$ evaluated with $T_{\rm PB}(\mathbf{R})$, the width (2.35σ) of the distribution of the $H(\mathbf{R})/N$ values is a measure of the quality of the variational wave function. In Fig. 1 we compare the distributions of the $H(\mathbf{R})/N$ obtained for an $N=20$ drop of liquid ^{4}He with the wave function Ψ_B [Eq. (3.1)], with and without the three-body correlation f_3. The inclusion of the f_3 in the wave function reduces the energy by a small amount, but it also reduces the width of the distribution by $\sim$40%. Typically, the difference between the exact GFMC energies[1] and the variational energies of liquid-^{4}He drops is reduced by a factor of 4 by including three-body correlations in the wave function.

Table I shows the CPU time required to do the present calculations using one processor of a Cray XMP-2 computer. We express all functions of r_i and r_{ij}, i.e., f_1, f_2, ξ_l, η, and ϕ_i, in terms of the cubic splines, and use the splines to evaluate the functions as needed. The Cray that was used does not have the hardware gather feature, and hence the time required to fetch the cubic-spline coefficients dominates the calculations of the Bose liquid drops. Evaluating the determinants[27] $\Phi_\uparrow$ and $\Phi_\downarrow$ is the most time-consuming part of the ^{3}He calculations. The last column of Table I shows the number of values of $H(\mathbf{R})$ needed to calculate the energy (per atom) with an error of $\sim$0.01 K. This number decreases with N since each $H(\mathbf{R})$ is an average of the kinetic and potential energies of N particles. It is obvious from Table I that calculations of drops containing several hundreds of bosons or up to 200 fermions are quite practical, whereas those drops with several hundreds of fermions are rather difficult with present-day computers.

B. The variational search

Minimizing the energy by varying the numerous parameters of the variational wave function is a major problem that is compounded by the fact that Monte Carlo evaluations have statistical errors. Furthermore, several pairs of parameters give correlated variations of the energy. For example, the effect of either increasing the α in f_2 or λ'_η in the backflow η, or of decreasing the depth V_ϕ of the Woods-Saxon well, is to increase the radius of the drop, and these parameters are strongly correlated. Similarly, variations of energy due to changes in r_ϕ and ω_ϕ are also correlated. The variational search procedure adopted was as follows. An initial guess of all the parameters was made, and two parameters were selected for study. About a dozen short calculations (with statistical error of 0.03 to 0.05 K in E/N) were done with various values of these parameters. A least-squares fit was used to approximate the results by a two-dimensional polynomial and obtain the best pair of parameter values. Another pair of parameters (possibly including one of the previous pair) would then be selected and the procedure repeated.

The smaller drops, which require less computing, were studied first, and more extensively, to establish the N-

TABLE I. Typical calculation times and rates. The listed CPU time, and average rate [in millions of floating point operations per second (MFLOP)] is for one step of the random walk. It includes $5N$ one-atom moves and an evaluation of $H(R)$ with $T_{\rm PB}$. These values are for a single processor of a Cray XMP-2 without hardware gather. The last column gives the number of steps needed to calculate E/N with a statistical error of 0.01 K.

System	N	CPU time (sec)	Rate (MFLOP)	$N_{\rm step}$
^{4}He	70	0.13	19	1700
^{4}He	240	1.0	26	1000
^{3}He	70	1.7	30	1000
^{3}He	240	68.0	90	700

dependence of the variational parameters. The variational search was much more limited for the larger drops; the parameters that had little N dependence were not varied. The parameters r_{ξ_l} and ω_{ξ_l} were found to have little N dependence, and their values, listed in Table II, are identical to those in the extended liquid.[6,8]

The wave functions that gave the lowest energies of the liquid-^{4}He drops are given in Table III. Both Ψ_A and Ψ_B give similar binding energies for the $N=70$ drop. The parameters of f_1 and ϕ_i are given in Tables IV and V, and those of f_2 are given in Table VI. We note that the α and ρ_L for the f_2 in extended liquid ^{4}He at equilibrium are, respectively, 3.46 Å^2 and 0.0219 Å^{-3}. Thus, it appears that the long-range part of f_2 in drops with a few hundred atoms is significantly different from that in the liquid. This result also implies that f_2 should be treated as a function of $\mathbf{r}_i$ and $\mathbf{r}_j$. Due to the strong correlations in the parameters of f_1 and f_2, and the limited accuracy of the present calculation, it is difficult to learn about the N dependence of α and ρ. Not much significance should be attached to the variations in α and ρ with N in Table VI. The parameters of $\tilde{f}_2$ for the $N=8$ ^{4}Ne system are

$$\kappa=0.0645\ \text{Å}^{-1},\quad C=2.8\ \text{Å},$$
$$r_\lambda=2.8\ \text{Å},\quad \omega_\lambda=0.95\ \text{Å}. \tag{4.10}$$

The values of λ_{ξ_l} in liquid-^{4}He drops are given in Table VII. They have an insignificant variation with N. The values of λ_{ξ_1} and λ_{ξ_0} in liquid ^{4}He are -0.165 and 0.0067 Å^{-2}. [It should be pointed out here that there is a typographical error in Ref. 6. The value of λ_0 (which is λ_{ξ_0} in the present notation) given in Table IV of Ref. 6 should be $+0.088\sigma^{-2}$ instead of $-0.044\sigma^{-2}$]. We note that the main $l=1$ term in f_3 is similar in the liquid and the drops. The sign of the $l=0$ term in drops is opposite to that in the liquid, and this may be associated with the large difference in the long-range behavior of f_2. Only the $l=1$ term is kept in the f_3 of liquid-^{3}He drops. We neglect its N dependence, and take λ_{ξ_1} equal to its value (-0.115 Å^{-2}) in the liquid. The lowest energies were obtained with the long-range backflow function [Eq. (3.15)] having $\lambda_\eta=0$ and $\lambda'_\eta=5.0$ Å^{-3}, and the $\eta(r)$ has little N dependence. Most calculations of the liquid use the short-range $\eta(r)$.

TABLE II. Values of r_{ξ_l} and ω_{ξ_l} in Å.

System	Parameter	Value
^{4}He	r_{ξ_1}	2.04
^{4}He	ω_{ξ_1}	1.05
^{4}He	r_{ξ_0}	2.81
^{4}He	ω_{ξ_0}	1.66
^{3}He	r_{ξ_1}	2.17
^{3}He	ω_{ξ_1}	1.15

More-refined calculations of liquid-^{4}He drops having $N\geq 70$ were attempted by modifying the wave function Ψ_A as follows:

$$\Psi_{A'}=\exp\left[\sum_{i=1}^{N}\tilde{u}_1(r_i)\right]\Psi_A\ , \tag{4.11}$$

$$\tilde{u}_1(r)=\frac{a+bx+cx^2}{\cosh(x)}\ , \tag{4.12}$$
$$x=(r^2-\gamma^2)/\tau^2\ .$$

The $\tilde{u}_1$ allows the f_1 to be varied in the region of $r=\gamma$ in an essentially arbitrary manner. The parameters of $\tilde{u}_1$ were searched by computing the gradient of $\langle H\rangle$:

$$\frac{\partial}{\partial p}\langle H\rangle=\left[2\left\langle\Psi\left|\left[\sum_i\frac{\partial}{\partial p}\tilde{u}_1(r_i)\right]H\right|\Psi\right\rangle-\frac{\hbar^2}{2m}\left\langle\Psi\left|\sum_i\left[\nabla_i^2\frac{\partial}{\partial p}\tilde{u}_1(r_i)+2\nabla_i\frac{\partial}{\partial p}\tilde{u}_1(r_i)\cdot\frac{\nabla_i\Psi}{\Psi}\right]\right|\Psi\right\rangle\right.$$
$$\left.-2\langle H\rangle\left\langle\Psi\left|\sum_i\frac{\partial}{\partial p}\tilde{u}_1(r_i)\right|\Psi\right\rangle\right]\Big/\langle\Psi\,|\,\Psi\rangle\ , \tag{4.13}$$

TABLE III. Best wave functions for liquid ^{4}He drops.

N	Wave function
8	Ψ_C
20, 40, 70	Ψ_B
70, 240	$\Psi_{A'}$
112, 728	Ψ_A

TABLE IV. Parameters of f_1 in Ψ_B and Ψ_C.

N	Type	r_ϕ (Å)	ω_ϕ (Å)	V_ϕ (K)
20	B	3.83	1.53	
40	B	5.11	1.28	
70	B	6.65	1.34	
70	A	7.92	1.66	−3.42
112	A	9.46	1.58	−3.30
240	A	12.78	1.53	−3.14
728	A	17.89	1.53	−3.12

TABLE V. Parameters of Woods-Saxon wells for liquid-^{3}He drops.

N	r_ϕ (Å)	ω_ϕ (Å)	V_ϕ (K)
20	7.2	1.33	−3.8
40	7.7	1.33	−6.8
70	9.0	1.33	−8.1
112	10.2	1.46	−9.8
168	11.5	1.46	−11.7
240	12.8	1.46	−14.6

TABLE VII. λ_{ξ_l} for liquid-^{4}He drops.

N	λ_{ξ_1} (Å^{-2})	λ_{ξ_0} (Å^{-2})
8	−0.165	−0.0067
20	−0.171	−0.0052
40	−0.171	−0.0052
70	−0.194	−0.0052
112	−0.184	−0.0052
240	−0.168	−0.0052
728	−0.168	−0.0052

where p denotes a parameter of $\tilde{u}_1(r)$. Formulas similar to Eq. (4.13) may be written for the second derivative of $\langle H \rangle$ with respect to the parameters and for derivatives with respect to the other parameters of Ψ. All of the required expectation values may be evaluated in the same random walk as is used to compute $\langle H \rangle$. We evaluated both the first and second derivatives for the parameters of $\tilde{u}_1$ and then used the second derivatives as a guide for how far to move in the direction indicated by the first derivatives. This $\Psi_{A'}$ gave lower energies for $N=70$ and 240; the parameters of $\tilde{u}_1$ for these drops are given in Table VIII. The analogous procedure could not be used when varying f_2 because our solutions of Eqs. (2.6) and (2.8) are not accurate enough to allow subsequent numerical differentiation with respect to the parameters α and ρ_L.

V. RESULTS

The lowest variational bounds obtained in this work are listed in Tables IX and X. The columns T/N and V/N in these tables give the kinetic and potential energies per atom; δ is the statistical error in E/N [Eq. (4.5)], and σ is the standard deviation of the $H(\mathbf{R})/N$ [Eq. (4.6)]. The $N=20$ ^{3}He drop is in a metastable state. Even though its energy is positive, we estimate from liquid-drop fits discussed later that its chemical potential is negative. The energy of this system goes through the minimum listed in Table X as r_ϕ is increased, and thus the central density of the drop is decreased. There obviously is another, somewhat uninteresting, minimum with $E/N=0$ in the limit $r_\phi \to \infty$, which corresponds to a gas of vanishingly small density. We note that there is an enormous cancellation between the kinetic and potential energies of small drops of liquid ^{3}He.

TABLE VI. Parameters of f_2.

	α (Å^2)		ρ_L (Å^{-3})	
N	^{4}He	^{3}He	^{4}He	^{3}He
20	0.653	1.24	0.012	0.009
40	1.182	1.24	0.0112	0.009
70	0.653	0.98	0.0135	0.0066
112	0.875	1.24	0.008	0.009
168		1.37		0.0066
240	0.849	1.70	0.0114	0.0066
728	1.176		0.0120	

The backflow correlations have a significant effect on the energy as can be seen from Table XI. Unfortunately these correlations make the ^{3}He drop calculations much more difficult. In the absence of these correlations, $\mathbf{r}_i' = \mathbf{r}_i$, and when a particle is moved only one column of the determinant $\Phi_\uparrow$ (or $\Phi_\downarrow$) changes. It is rather simple to calculate the change in the determinant in this case without recalculating the entire determinant.[28] However, when we consider backflow correlations, all $\mathbf{r}_j'$ change when a single particle is moved [Eq. (2.15)], and both the determinants $\Phi_\uparrow$ and $\Phi_\downarrow$ have to be recomputed.

The $N=8$ ^{3}He system is unbound but the ^{4}He system is bound. Several calculations were made to find if this is due to the statistics or the mass difference between the atoms. In Table XII we list the energies obtained for the $N=8$ systems of ^{4}He and ^{3}He atoms with both Bose and Fermi statistics. The ^{3}He Bose system is rather weakly bound, and so is the ^{4}He Fermi system. Thus, both statistics and mass difference have a comparable effect; similar results are obtained for larger drops and the liquids.[9] The exact GFMC results for the ^{4}He Bose system[1] and the GFMC transient estimate for ^{4}He Fermi system[29] are also listed in Table XII. We note that the fractional error in the variational calculations is much larger for the Fermi system. This is principally due to the smaller binding energy of the Fermi system; the absolute errors are comparable. Schmidt[30] is carrying out a GFMC (fixed nodes) calculation of the $N=70$ ^{3}He drop; his preliminary result for E/N is −0.4 K which is below our variational result by 0.1 K. The GFMC and variational E/N for the $N=70$ ^{4}He drop are[2] −3.12 and −3.03 K, respectively.

The density distributions of the ^{4}He drops are given in Fig. 2, while those of the ^{3}He drops are given in Fig. 3. We note that the central density of $N=20$ ^{3}He drops is less than half of the liquid ρ_0 (0.0165 Å^{-3}). The average central density of the ^{3}He drops rises rather slowly with N, and that of the $N=240$ drop is $\sim$0.016 Å^{-3}. The thickness of the surface of the $N=168$ and 240 drops is $\sim$8 Å. In contrast, the central density of ^{4}He drops is

TABLE VIII. Parameters of $\tilde{u}_1$.

N	γ (Å)	τ (Å)	a	b	c
70	1.92	3.58	−0.1	−0.05	−0.08
240	1.92	3.58	−0.2	−0.05	−0.08

TABLE IX. Energies per atom of ^{4}He drops in K. [Numbers in parentheses indicate the one-sigma errors in the last digits of the quoted values. The column labeled σ gives the standard deviation defined in Eq. (4.6).]

N	Ψ	T/N (K)	V/N (K)	$E/N(\delta)$ (K)	σ (K)	N_{steps}
8	C	2.48	−3.08	−0.5989(8)	0.41	260 000
20	B	4.52	−6.09	−1.5734(13)	0.43	110 000
40	B	6.28	−8.66	−2.389(2)	0.49	60 000
70	B	7.15	−10.18	−3.031(3)	0.43	19 000
70	A'	7.04	−10.07	−3.028(3)	0.44	19 000
112	A	7.81	−11.31	−3.498(5)	0.44	8000
240	A'	8.71	−12.91	−4.193(5)	0.33	4300
728	A	9.69	−14.63	−4.938(5)	0.20	1565
∞		14.72[a]	−21.65[a]	−6.93(5)[a]		

[a]Reference 6.

80% of the liquid ρ_0 (0.022 Å^{-3}) for $N=20$ and reaches the liquid value by $N=70$. The thickness of the surface of ^{4}He drops with $N \geq 112$ is ~ 7 Å. The density distributions of $N=8$ systems are given in Fig. 4.

The density distributions of uncorrelated ^{3}He drops, obtained with just the Slater determinants $\Phi_\uparrow$ and $\Phi_\downarrow$, without correlations or backflow, are given in Fig. 5. We note that the correlations have a very large effect on $\rho(r)$. The uncorrelated drops have large central densities, and significant shell oscillations. The correlations reduce the central density, and also smooth out shell oscillations in $\rho(r)$. A similar result is obtained for the ^{4}He drops (Fig. 6); the density distribution corresponding to $f_1(r)$ has a much smaller rms radius than that of the correlated drop.

The last filled shell of Fermi ^{3}He drops with $N=20$, 70, and 168 contain even-l orbits. The s-orbital wave functions have maxima at $r=0$, and hence the $N=20$, 70, and 168 body drops can have a bump in $\rho(r)$ at $r=0$ due to shell structure. On the other hand, the $\rho(r)$ of drops with $N=8$, 40, 112, and 240 can have a dip at $r=0$ because the last filled shell has only odd-l orbits for which the wave function is zero at $r=0$. These bumps and dips are quite noticeable in the density distributions obtained from the uncorrelated Slater determinants (Fig. 5). They have also been observed in the charge densities of atomic nuclei,[31] with an amplitude that is smaller than that predicted by a Slater determinant obtained from a Woods-Saxon well. The densities of $N=8$ (Fig. 4) and 112 (Fig. 3) drops show the expected dip at $r=0$, while that of $N=70$ (Fig. 3) has a bump. The densities of $N=20$ and 40 drops (Fig. 3) do not have any significant structure at $r=0$, while statistical uncertainties are too large in the $\rho(r)$ of $N=168$ and 240 drops (Fig. 3) to draw definite conclusions. Experimentally the shell structure is much more visible in density differences of adjacent nuclei;[32] we are making a detailed study of the density differences of adjacent drops.

The density distributions obtained with the two wave functions ($\Psi_{A'}$ and Ψ_B) that give similar energies for the $N=70$ ^{4}He drop are shown in Fig. 6, along with the single-particle density ($f_{1,x}^2$) of the uncorrelated wave functions obtained by setting $f_2=f_3=1$. This comparison shows the uncertainties in extracting the central densities and surface thicknesses from variational calculations. In GFMC calculations,[2] the central density also requires a very large number of interactions to stabilize because the energy is relatively insensitive to $\rho(r\sim 0)$. The $\rho(r)$ obtained with Ψ_B is more like a conventional liquid drop with an approximately uniform central density, while that from $\Psi_{A'}$ does not appear to have any central plateau.

It is rather easy to produce structure in the density distribution of liquid-^{4}He drops at the cost of little excitation energy. The energies and density distributions obtained for the $N=20$ ^{4}He drop, with five different wave functions, are shown in Fig. 7. The wave function corresponding to the dashed curve is of the type Ψ_B; its parameters

TABLE X. Energies per atom of ^{3}He drops in K. (Numbers in parentheses indicate the same as for Table IX.)

N	T/N (K)	V/N (K)	$E/N(\delta)$ (K)	σ (K)	N_{steps}
20	1.87	−1.67	+0.206(7)	0.44	4000
40	3.86	−3.89	−0.036(2)	0.35	25 000
70	5.06	−5.33	−0.275(2)	0.34	20 000
112	5.79	−6.25	−0.460(3)	0.31	8500
168	6.56	−7.18	−0.618(6)	0.30	2200
240	7.07	−7.81	−0.743(13)	0.26	400
∞	12.28[a]	−14.64[a]	−2.36(10)[a]		

[a]Reference 8.

TABLE XI. Energy per atom (K) of ^{3}He drops with and without backflow correlations. (Numbers in parentheses indicate the one-sigma errors in the last digits.)

	E/N (K)	
N	Without	With
40	$\sim+0.1$	$-0.036(2)$
70	$-0.10(1)$	$-0.275(2)$
112	$-0.27(1)$	$-0.460(3)$

and the properties calculated with it are listed in the tables. The $f_1(r)$ for the other curves contain an additional factor that was designed to modify the central density. The central density can be changed by $\pm 20\%$ ($\pm 40\%$) with only a 1% (4%) increase of E/N.

Calculations were also carried out to test the sensitivity of the energy to the parameters of f_2 and f_3 for the $N=112$ drop. For example, the energy obtained with the f_3 of the equilibrium liquid which has $\lambda_{\xi_1}=-0.165$ and $\lambda_{\xi_0}=0.0067$ Å^{-2} and an f_2 with $\rho_L=0.016$ Å^{-3} and $\alpha=2.09$ Å^2 is $-3.466(5)$ per atom compared to $-3.498(5)$ obtained with the parameters of Tables VI and VII. The f_1 used in this wave function has a significantly shorter range to compensate for the stronger repulsion caused by the larger α; however, the density is very similar to that shown in Fig. 2.

A rather interesting $\rho(r)$ obtained with a $\Psi_{A'}$ wave function for the $N=728$ drop is shown in Fig. 8. The $\exp[2\tilde{u}_1(r)]$ used in this wave function is also shown in the figure; it has a sharp peak at 14 Å. The resulting $\rho(r)$ also has a sharp peak at 14 Å, and oscillations with a wavelength of 3 Å in the region $6<r<17$ Å. The wave number of these oscillations (2 Å^{-1}) corresponds to that of rotons in the liquid. The energy obtained with this wave function is 1.2% higher than the best variational energy; this corresponds to a total increase of only 41.5 K for the drop. There is a large increase (103 K) in the kinetic energy which is partly compensated by an increase in the potential energy.

The calculated binding energies of the $N>20$ drops can be reproduced with the liquid-drop formulas containing volume, surface, and curvature terms:

$$E(N)/N=E_v+E_s x+E_c x^2\,, \tag{5.1}$$

where

$$x=N^{-1/3}\,. \tag{5.2}$$

Typical fits are shown in Table XIII. Ideally the value of

TABLE XII. Energy per atom (K) of various $N=8$ systems. (Numbers in parentheses indicate the one-sigma errors in the last digits.)

	^{4}He(var) (K)	^{4}He(GFMC) (K)	^{3}He(var) (K)
Bose	$-0.5989(8)$	$-0.6165(6)$	$-0.0842(6)$
Fermi	$-0.1743(13)$	$-0.205(8)$	unbound

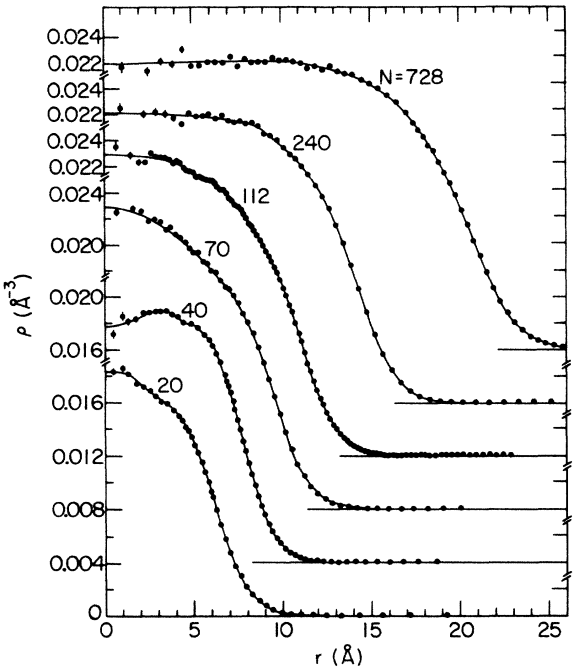

FIG. 2. Density profiles for the ^{4}He drops. The error bars show the Monte Carlo binning of the densities; the curves are drawn to guide the eye. The curves are labeled with the number of atoms in the drops.

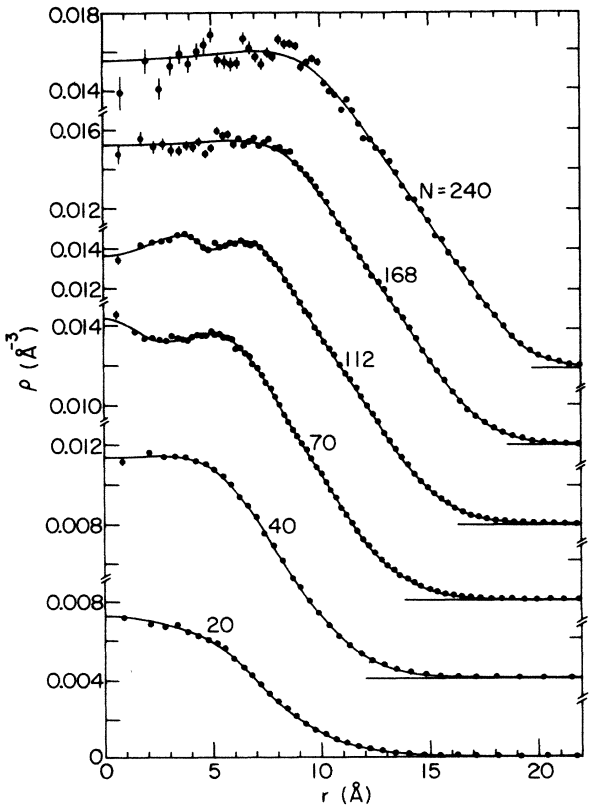

FIG. 3. Density profiles for the ^{3}He drops; see Fig. 2.

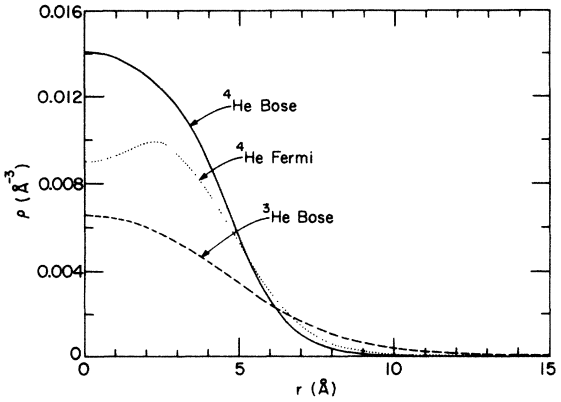

FIG. 4. Density profiles for drops with eight atoms: Solid curve, mass 4, Bose statistics; dashed curve, mass 3, Bose statistics; dotted curve, mass 4, Fermi statistics.

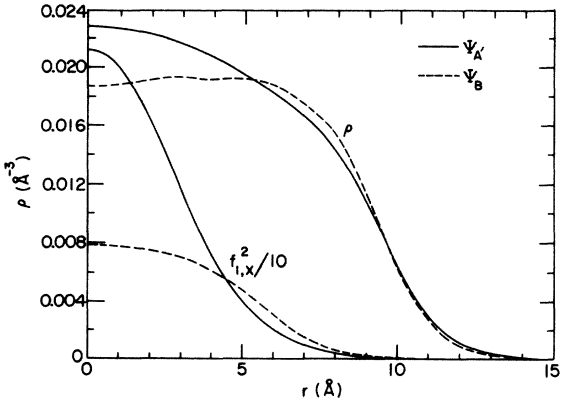

FIG. 6. Density distributions (top curves) and single-particle densities divided by 10 (bottom curves) for the two 70-atom ^{4}He wave functions. The solid curves are for Ψ_A, and the dashed for Ψ_B.

χ^2/N_f should be near 1. From this consideration we choose the fits using $N=40$–728 ^{4}He drops and $N=20$–240 ^{3}He drops as most satisfactory. These are used in the following discussion. The energies of the drops and the fitted curves are shown in Fig. 9.

The first coefficient E_v gives the energy per atom of the liquid. The value of E_v obtained for ^{4}He is in good agreement with the variational calculations of the liquid[6] with HNC summation methods, while that for ^{3}He is above the -2.36 K obtained with FHNC methods.[8] This difference is probably due to the inaccuracy of the FHNC calculations of Ref. 8. Our value of E_v is in good agreement with the more recent variational Monte Carlo calculations[17] of liquid ^{3}He.

The second coefficient E_s is related to the surface tension t,

$$t=E_s/(4\pi r_0^2)\ , \tag{5.3}$$

where r_0 is the unit radius of the liquid,

$$\frac{4\pi}{3}r_0^3\rho_0=1\ . \tag{5.4}$$

The values of t obtained from E_s are 0.29 and 0.13 K Å^{-2} for ^{4}He and ^{3}He, respectively, and the experimental values are 0.27 and 0.11 K Å^{-2}. It thus appears that the surface tension is overestimated in the present work. We recall that the $t=0.30$ K Å^{-2}, obtained for ^{4}He by fitting the GFMC energies of $N=20$–112 drops with the formula (5.1), is also too high.[1] A lower value of 0.28 K Å^{-2} is obtained when terms of order x^3 and x^4 are included in the formula. Thus, it is not clear if the present overestimate of t is due to inadequacies in the calculation of $E(N)$, in extracting t from the $E(N)$, or in the interaction itself.

Normally one would expect the curvature correction to the energy of a convex surface to be positive, and in fact, if one includes the x^3 and x^4 terms in the liquid-drop energy formula,[1] the E_c of ^{4}He drops becomes positive. Thus the negative E_c found in the present fits has little physical significance. The E_c is primarily determined by the energies of small drops whose central density is much

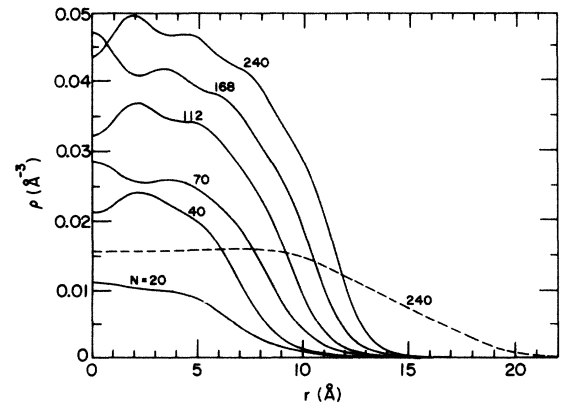

FIG. 5. Density distribution of the uncorrelated Slater determinants for the ^{3}He drops. The curves are labeled with the number of atoms in each drop. The dashed curve is the density distribution of the full correlated wave function for the 240-atom drop.

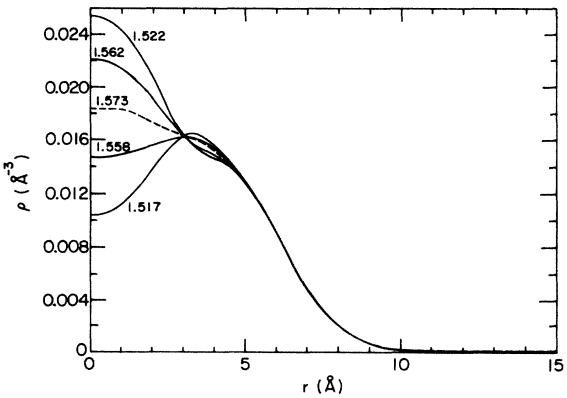

FIG. 7. Density distributions for 20-atom ^{4}He drops. The dashed curve is for the wave function Ψ_B of the tables. The solid curves are modifications of Ψ_B as described in the text. The curves are labeled with the binding energy per atom $(-E/N)$.

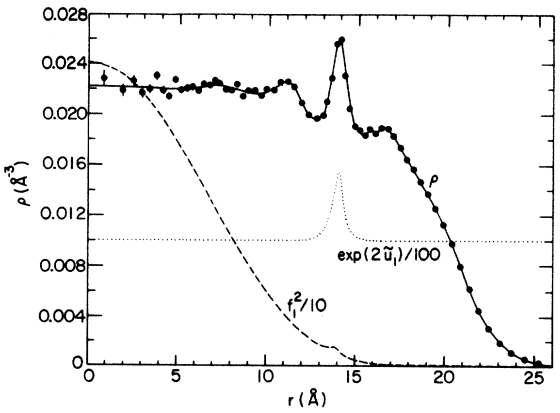

FIG. 8. Density distribution for the 728-atom ^{4}He drop with a forced peak near the surface. The dashed curve is the single-particle density divided by 10. The dotted curve is $\exp(2\tilde{u}_1)$ divided by 100.

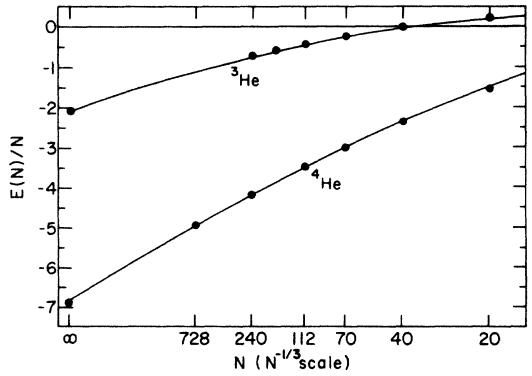

FIG. 9. E/N for the ^{3}He and ^{4}He drops. The abscissa is N on an $N^{-1/3}$ scale. The curves are from rows 2 and 3 of Table XIII.

less than that of the liquid.

The unit radii $r_0(N)$ are defined as

$$r_0(N)=[\tfrac{5}{3}\langle r^2(N)\rangle]^{1/2}/N^{1/3}\,, \tag{5.5}$$

where $\langle r^2(N)\rangle$ is the mean-square radius of an N-body drop. The values of $r_0(N)$ for both ^{4}He and ^{3}He drops are given in Table XIV. The rms radii of the drops have negligible statistical uncertainty resulting from Monte Carlo sampling. The main error in $\langle r^2(N)\rangle$ comes from the uncertainty in choosing the best variational wave functions. In particular, the uncertainty in the radius of the $N=20$ ^{3}He (metastable) drop is large because the energy does not change significantly with a $\pm 10\%$ variation in radius. The energies of larger drops are much more sensitive to their radii, and thus their radii are much better determined.

The unit radius $r_0(\infty)$ of the liquid can be extracted by fitting the $r_0(N)$ by a polynomial in $N^{-1/3}$. A fit to the calculated unit radii of $N=40$–728 ^{4}He drops with a second-order polynomial gives $r_0(\infty)=2.21(4)$ Å for liquid ^{4}He, in good agreement with the experimental value of 2.22 Å as well as with the GFMC value for the Aziz potential. The quoted error of $r_0(\infty)$ is an estimate based on both the variational and extrapolation errors. Fits to unit radii of ^{3}He drops having $N=40$–240 give $r_0(\infty)=2.5(1)$ Å in agreement with the experimental value of 2.43 Å. We note that the central densities of $N=240$ and 728 ^{4}He drops (Fig. 2) and $N=240$ ^{3}He drop (Fig. 3) are compatible with these values of $r_0(\infty)$.

VI. DISCUSSION

We have made VMC calculations of the ground states of small- to moderate-sized drops of liquid ^{4}He and ^{3}He. Comparisons with GFMC calculations show that our binding energies are typically 0.1 K per atom too low. There is unfortunately no suitable experimental data to which these calculations can be compared. A mass spectrometer experiment[33] has reported the observation of magic numbers for both ^{4}He and ^{3}He drops and also ^{3}He drops containing as few as four atoms. However, the drops are charged and may be fragmented in the mass spectrometer. Detailed GFMC calculations[34] for neutral ^{4}He drops show only a smooth energy versus drop-size relation. The very small binding energy for eight ^{4}He atoms with Fermi statistics obtained with GFMC makes it certain that eight ^{3}He atoms are not bound. For these reasons, we agree with the conclusions of Ref. 34, that the charge on the drops has significantly altered their properties. Macroscopic liquid drops having more than 10 000 helium atoms have been used in experiments.[35] Experimental studies of small neutral drops would be very interesting. In particular, there is the question of what is the smallest number of ^{3}He atoms that will form a bound state. Our calculations suggest that this number is just slightly less than 40. However, if our energy for 40 ^{3}He atoms is 0.1 K too high, the number will be close to 30.

There is an interesting contrast between studies of liquid-helium drops and nuclei. By fitting liquid-drop expansions to the drop energies, we can obtain binding-

TABLE XIII. Liquid-drop energy fits. The coefficients of the polynomial defined in Eq. (5.1) are given. The last column gives χ^2 per degree of freedom.

System	Range	E_v	E_s	E_c	χ^2/N_f
^{4}He	$N=20$–728	−7.00	19.6	−13.3	9.0
^{4}He	$N=40$–728	−6.85	18.2	−9.9	2.0
^{3}He	$N=20$–240	−2.09	9.9	−9.9	2.9
^{3}He	$N=40$–240	−1.90	8.3	−6.4	0.36
^{3}He	$N=70$–240	−2.09	10.0	−10.5	0.04

TABLE XIV. $r_0(N)$ of liquid drops in Å. The two values for $N=70$, ^{4}He correspond to Ψ_B and $\Psi_{A'}$.

N	$r_0(N)$ (Å) ^{4}He	^{3}He
20	2.77	
40	2.54	3.29
70	2.48, 2.50	3.01
112	2.43	2.89
168		2.78
240	2.37	2.71
728	2.32	

energy and surface-tension values for the infinite liquid. These are the only comparisons we can make with known experimental values. In contrast, the binding energies of nuclei are known experimentally and must be extrapolated to obtain the experimentally inaccessible nuclear matter properties. In Fig. 9 it can be seen that a curvature term is important to this extrapolation. However, such a term is rarely used for nuclei due to the complications of other effects such as the symmetry term.

ACKNOWLEDGMENTS

We wish to thank J. J. Dongarra, R. M. Panoff, K. E. Schmidt, and J. G. Zabolitzky for useful discussions. The calculations were made possible by a grant of computer time on the Energy Research Cray of the U.S. Department of Energy. This work is supported by the U.S. Department of Energy, Nuclear Physics Division, Contract No. W-31-109-ENG-38 and Materials Science Division, Contract No. DE-AC02-76ER01198, and by the National Science Foundation, Grant No. PHY84-15064.

[1]R. A. Aziz, V. P. S. Nain, J. S. Carley, W. L. Taylor, and G. T. McConville, J. Chem. Phys. **70**, 4330 (1979).
[2]V. R. Pandharipande, J. G. Zabolitzky, S. C. Pieper, R. B. Wiringa, and U. Helmbrecht, Phys. Rev. Lett. **50**, 1676 (1983).
[3]S. Stringari, Phys. Lett. **107A**, 36 (1985).
[4]S. C. Pieper, R. B. Wiringa, and V. R. Pandharipande, Phys. Rev. B **32**, 3341 (1985).
[5]C. C. Chang and M. Cohen, Phys. Rev. B **11**, 1059 (1975).
[6]Q. N. Usmani, S. Fantoni, and V. R. Pandharipande, Phys. Rev. B **26**, 6123 (1982).
[7]K. Schmidt, M. H. Kalos, M. A. Lee, and G. V. Chester, Phys. Rev. Lett. **45**, 573 (1980).
[8]E. Manousakis, S. Fantoni, V. R. Pandharipande, and Q. N. Usmani, Phys. Rev. B **28**, 3770 (1983).
[9]K. E. Schmidt, M. A. Lee, M. H. Kalos, and G. V. Chester, Phys. Rev. Lett. **47**, 807 (1981).
[10]C. E. Campbell and E. Feenberg, Phys. Rev. **188**, 396 (1969).
[11]L. J. Lantto and P. J. Siemens, Phys. Lett. **68B**, 308 (1977).
[12]M. H. Kalos, M. A. Lee, P. A. Whitlock, and G. V. Chester, Phys. Rev. B **24**, 115 (1981).
[13]Q. N. Usmani, B. Friedman, and V. R. Pandharipande, Phys. Rev. B **25**, 4502 (1982).
[14]G. V. Chester and L. Reatto, Phys. Lett. **22**, 276 (1966).
[15]C. C. Chang and C. E. Campbell, Phys. Rev. B **15**, 4238 (1977).
[16]R. P. Feynman and M. Cohen, Phys. Rev. **102**, 1189 (1956).
[17]P. A. Whitlock and R. M. Panoff, Los Alamos National Laboratory Report No. LA-10227-C, 1984 (unpublished), Vol. 2, p. 430.
[18]R. M. Panoff (private communication).
[19]J. Lomnitz-Adler, V. R. Pandharipande, and R. A. Smith, Nucl. Phys. **A361**, 399 (1981).
[20]R. B. Wiringa, S. C. Pieper, and V. R. Pandharipande (unpublished).
[21]E. Krotscheck, G.-X. Qian, and W. Kohn, Phys. Rev. B **31**, 4245 (1985).
[22]A. Bohr and B. R. Mottelson, *Nuclear Structure* (Benjamin, New York, 1969), Vol. 1.
[23]M. Manousakis and V. R. Pandharipande, Phys. Rev. B **30**, 5062 (1984).
[24]N. Metropolis, A. W. Rosenbluth, M. N. Rosenbluth, A. M. Teller, and E. Teller, J. Chem. Phys. **21**, 1087 (1953).
[25]H. W. Jackson and E. Feenberg, Ann. Phys. (N.Y.) **15**, 266 (1961).
[26]J. G. Zabolitzky, Phys. Rev. A **16**, 1258 (1977).
[27]J. J. Dongarra and S. C. Eisenstat, ACM Trans. Math. Software **10**, 221 (1984). The Cray subroutine SGEMV was used for the vector-matrix operations; ISAMAX was used to find pivot elements.
[28]D. Ceperley, G. V. Chester, and M. H. Kalos, Phys. Rev. B **16**, 3081 (1977).
[29]U. Helmbrecht and J. G. Zabolitzky, Nucl. Phys. **A442**, 109 (1985).
[30]K. E. Schmidt (private communication).
[31]J. W. Negele and D. Vautherin, Phys. Rev. C **5**, 1472 (1972).
[32]J. M. Cavedon *et al.*, Phys. Rev. Lett. **49**, 978 (1982).
[33]P. W. Stephens and J. G. King, Phys. Rev. Lett. **51**, 1538 (1983).
[34]R. Melzer and J. G. Zabolitzky, J. Phys. A **17**, L565 (1984).
[35]J. Gspann and H. Vollmar, J. Low Temp. Phys. **45**, 343 (1981).